

PCCP

Accepted Manuscript



This is an *Accepted Manuscript*, which has been through the Royal Society of Chemistry peer review process and has been accepted for publication.

Accepted Manuscripts are published online shortly after acceptance, before technical editing, formatting and proof reading. Using this free service, authors can make their results available to the community, in citable form, before we publish the edited article. We will replace this *Accepted Manuscript* with the edited and formatted *Advance Article* as soon as it is available.

You can find more information about *Accepted Manuscripts* in the [Information for Authors](#).

Please note that technical editing may introduce minor changes to the text and/or graphics, which may alter content. The journal's standard [Terms & Conditions](#) and the [Ethical guidelines](#) still apply. In no event shall the Royal Society of Chemistry be held responsible for any errors or omissions in this *Accepted Manuscript* or any consequences arising from the use of any information it contains.

ARTICLE

Painting Biological Low-Frequency Vibrational Modes from Small Peptides to Proteins

Cite this: DOI: 10.1039/x0xx00000x

S. Perticaroli,^{abc*} D. Russo,^{de*} M. Paolantoni,^f M. A. Gonzalez,^g P. Sassi,^f J. D. Nickels,^{ac} G. Ehlers,^h L. Comez,^{ij} E. Pellegrini,^g D. Fioretto,^{jk} A. Morresi,^f

Received 00th January 2012,

Accepted 00th January 2012

DOI: 10.1039/x0xx00000x

www.rsc.org/

Protein low-frequency vibrational modes are an important portion of a proteins' dynamical repertoire. Yet, it is notoriously difficult to isolate specific vibrational features in the spectra of proteins. Given an appropriately chosen model peptide, and using different experimental conditions, we can simplify the system and gain useful insights into the protein vibrational properties. Combining neutron scattering, depolarized light scattering, and molecular dynamics simulations, we analyse the low frequency vibrations of biological molecules, comparing the results from a small globular protein, lysozyme, and an amphiphilic peptide, NALMA, both in solution and in powder states. Lysozyme and NALMA present similar spectral features in the frequency range between 1 and 10 THz. With the aid of MD simulations, we assign the spectral features to methyl groups' librations (1–5 THz) and hindered torsions (5–10 THz) in NALMA. Our data also show that, while proteins display boson peak vibrations in both powder and solution forms, NALMA exhibits boson peak vibrations in powder form only. This provides insight into the nature of this feature, suggesting a connection of BP collective motions to a characteristic length scale of heterogeneities present in the system. These results provide context for the use of model peptide systems to study protein dynamics; demonstrating both their utility, and the great care that has to be used in extrapolating results observed in powder to solutions.

Introduction

Proteins experience a wide variety of vibrational motions, ranging from femtosecond high-frequency localized oscillations to low-frequency collective modes occurring at $\sim 10^{-11}$ s timescale¹. These low-frequency modes are increasingly being recognized as important players in the dynamical activity of proteins, with recent experimental results connecting changes in low-frequency vibrations to ligand binding in the enzyme dihydrofolate reductase² and lysozyme³. More generally, the low-frequency motions are believed to facilitate larger conformational translations and to determine the probability of barrier crossing within the transition state^{4, 5}. They may also contribute to the reaction coordinates of the functional motions in active proteins⁶. For a variety of reasons, modern biophysical methods often force researchers to conduct their experiments far from biologically relevant conditions, and extrapolate results to represent the full system⁷. It is because of this that important studies are being conducted on proteins in the powder state and on protein-analogues such as peptides; and relatively few studies have explored these low-frequency vibrations for proteins in solution^{3, 8-11}.

Low-frequency vibrations (<10 THz) can be experimentally studied with a range of techniques, including; depolarized light scattering (DLS), its time-domain counterpart, optical Kerr effect (OKE), and neutron scattering (NS) spectroscopies^{3, 8, 9, 11-19}. These are sensitive to both solute and solvent dynamics and are well suited to probe biomolecule-water and water-water

hydrogen bond interactions^{8, 11, 13, 15, 20, 21}. A great advantage of the MD simulation approach is that it allows one to describe, with atomic resolution, the origin of vibrational modes through a reliable assessment of the contribution of each biomolecule atom to the vibrational density of states²².

NS also provides the unique opportunity to isolate the dynamics of the biomolecule from those of the solvent based on isotopic sensitivity. This is accomplished by using a hydrogenated biomolecule in deuterated water (D₂O). The deuterium has a significantly smaller incoherent scattering cross-section relative to hydrogen. The main contribution to the scattered intensity then arises from hydrogen atoms in the biomolecule. In proteins, a large fraction of the non-exchangeable hydrogen atoms belong to methyl groups^{14, 23}. Typically found in the hydrophobic core of proteins, methyl groups are often used as probes for structure and dynamics²⁴⁻²⁷. They are also located near centers of biological activity in enzymes such as active sites and hinges where they are hypothesized to act as intrinsic plasticizers to facilitate protein dynamics, flexibility and activity²⁸. Neutron scattering spectra display modes related to methyl group vibrations in the low-frequency regime. These motions appear to be highly localized to the CH₃ groups situated in the protein side chains²⁹. They are also thought to be sensitive to their local microenvironment²⁹⁻³³.

The other region of interest in the low-frequency spectra of proteins using neutron scattering (NS) and depolarized light scattering (DLS) is a broad band occurring in an energy range

of ~350 GHz and ~1 THz, which is sensitive to temperature and hydration conditions³⁴. This is generally interpreted as the Boson peak (BP)^{8, 9, 11, 12, 21, 23, 34-40}. On the other hand, this feature is sometimes assigned to either underdamped or overdamped vibrational modes^{3,9}. The BP stems for collective vibrations involving a great number of atoms^{8, 9, 11, 12, 21, 23, 34, 36, 37, 39, 41, 42} distributed through the whole protein^{34, 39}. These motions are common in glass-forming systems⁴³⁻⁴⁵ and likely have a shared physical origin with those observed in proteins and amino acid mixtures. This is suggested by observations of a universal BP spectral shape which scales with peak frequency and amplitude³⁷. Models of the BP vibrations suggest that this origin is connected to scattering from nanometer scale heterogeneities. In proteins, these heterogeneities emerge on the (~1–2.5 nm) length scale, which is comparable to the dimension of protein secondary structural units, such as α -helices and β -sheets. This connection has spawned further studies relating BP frequency to the rigidity of these structural units^{23, 36, 37}.

In order to better understand low frequency vibrational motions in proteins, we have developed the comparison of a widely studied globular protein, lysozyme, and the amphiphilic peptide N-Acetyl-Leucine-MethylAmide (NALMA). Ever since lysozyme was discovered by Fleming in 1922, this protein has emerged as a model for investigations on protein structure, dynamics and function. The short peptide NALMA, has previously been the object of a variety of studies as a protein analogue^{13, 15, 22, 46, 47}. With two methyl groups located in a hydrophobic side chain, and an additional two methyl groups directly bound to the hydrophilic backbone, NALMA has been demonstrated to mimic important characteristics of proteins. This is also true in the context of dynamical studies where the NALMA shows a simplified version of the low-frequency vibrations found in proteins^{13, 15} as well as the effects of proteins on hydration water dynamics^{13, 15, 46, 47}.

Using DLS and NS experiments, together with MD simulations, we have analyzed the low frequency vibrations of these systems for the solution state and dry powder form. We make site-specific assignments for the vibrational density of state for NALMA below 10 THz and characterize methyl groups picosecond and femtosecond dynamics. Our data illustrates the different sensitivities that the DLS and NS techniques to low frequency vibrations, showing that methyl group torsions are not Raman active. And finally, our experiments clearly demonstrate that the BP feature, universally present for protein systems in both powder and solution states, is not observed for model peptides in solution. This is consistent with a molecular origin of the BP collective motions requiring a length scale on the order of nanometers, far larger distances than isolated NALMA molecules in solution. This comparison of results obtained through the adoption of reductionist approaches and sample restricted techniques, provides a context for the interpretation of a wide range of experimental results. We show that such data can be highly informative, despite having been obtained in conditions far removed from the in vivo reality.

Materials and methods

DLS and NS experiments

NALMA (MW=186.25Da) was purchased from Bachem, and lysozyme from chicken egg white (MW 14.4 kDa) and D₂O were Sigma-Aldrich products. Aqueous solutions of NALMA and lysozyme used in DLS experiments were prepared at a

range of concentrations from 12–283 mg solute/ml H₂O. All DLS spectra, including those of the neat solvent and of NALMA and lysozyme dry powders, were collected at 298K. A Coherent-Innova 90 Ar⁺ laser operating on a single mode of the $\lambda = 514.5$ nm line with power 300 mW was used as light source. The depolarized scattered radiation was analyzed between 30 GHz to 36 THz by a Jobin-Yvon U1000 double monochromator, with a resolution of 15 GHz in the 30 GHz – 1.8 THz range and a resolution of 30 GHz from 0.12 to 36 THz⁸ in the case of samples in solution. Spectra on the powders were collected between 400 GHz and 15 THz.

Neutron scattering experiments were performed on the Cold Neutron Chopper Spectrometer (CNCS)⁴⁸ at Spallation Neutron Source (SNS), Oak Ridge (TN), using an incident energy of 3 meV and an elastic resolution of ~50 μ eV (~20 ps). The experimental setup provided access to a Q range from 0.2 to 4 \AA^{-1} . All exchangeable hydrogen atoms in NALMA and lysozyme were exchanged to deuterium by dissolving the solutes in 99.9% D₂O at 10 mg/ml, for ~8 hours at 4°C, and then lyophilized. Such process was repeated twice. Portions of these peptide and protein powders were directly used as dry samples. Residual water content of these dry powders is estimated to be less than 3% and 5% by weight for NALMA and lysozyme respectively⁴². The absence of sharp Bragg peaks in the Static Structure Factor obtained from our neutron experiments confirms that our samples were amorphous (Fig. S1 in Electronic Supplementary Information).

Other aliquots of these lyophilized powders were employed to prepare solutions at 100 mg solute/ml D₂O concentration. All NS measurements, including those on neat D₂O, were carried out at 295K. The data were reduced using DAVE software package⁴⁹ and VDOSs of NALMA powders were calculated as in ref³⁷. NS spectra were summed over all Q^{37, 42}.

Data are presented in terms of the imaginary part of the dynamic susceptibility, $\chi''(\nu)$, a formalism chosen because it allows for a direct comparison of DLS and NS spectra^{42, 50}. NS experiments directly measure the vibrational density of states, $g(\nu)$, without any weighting coefficient, through the measurement of the dynamic structure factor $S(Q, \nu)$ ^{42, 51}:

$$\chi''_{NS}(Q, \nu) \propto \frac{S(Q, \nu)}{n_B(\nu)} \propto \frac{g(\nu)}{\nu} \quad (1)$$

where, $n_B(\nu)$ is the Bose-Einstein occupation number $n_B(\nu) = [\exp(h\nu/kT) - 1]^{-1}$. The imaginary part of the dynamic susceptibility of DLS spectra, on the other hand, is calculated from the experimental intensity $I(\nu)$ which is related to $g(\nu)$ by the relation:

$$\chi''_{DLS}(\nu) \propto \frac{I(\nu)}{n_B(\nu)+1} \propto \frac{C(\nu)g(\nu)}{\nu} \quad (2)$$

where $C(\nu)$ is the photon-phonon or Raman light-vibration coupling coefficient.

Finally, we have also used the spectral density representation, I_n , to present the spectra of NALMA and lysozyme powders since such formalism conveniently enhances and isolates the BP feature³⁶. This is calculated as the ratio $\chi''(\nu)/\nu$ for both NS and DLS datasets.

MD simulations

Molecular dynamics (MD) simulations have been performed on NALMA powders, using the COMPASS27 force field and the FORCITE module inside the Materials Studio Modelling Environment (v. 5.0) from Accelrys, Inc.⁵². We explored two hydration levels, $h=0$ (72 NALMA molecules) and $h=0.68$ by weight (72 NALMA molecules / 504 water molecules) at 298K. Both systems were equilibrated in the NVT ensemble for 260 ps (using a time step of 1.0 fs), using Berendsen's thermostat

with a relaxation time constants of 1.0 ps; and fixing the Cartesian positions of the central carbon atom $C\alpha$. After the removal of this constraint, production runs of 1 ns duration were carried out in the NVT ensemble using Berendsen's

thermostat, with a relaxation time constant of 1.0 ps. The standard Ewald summation method (with a cutoff radius $R=10$ Å) was used to treat the electrostatic interactions.

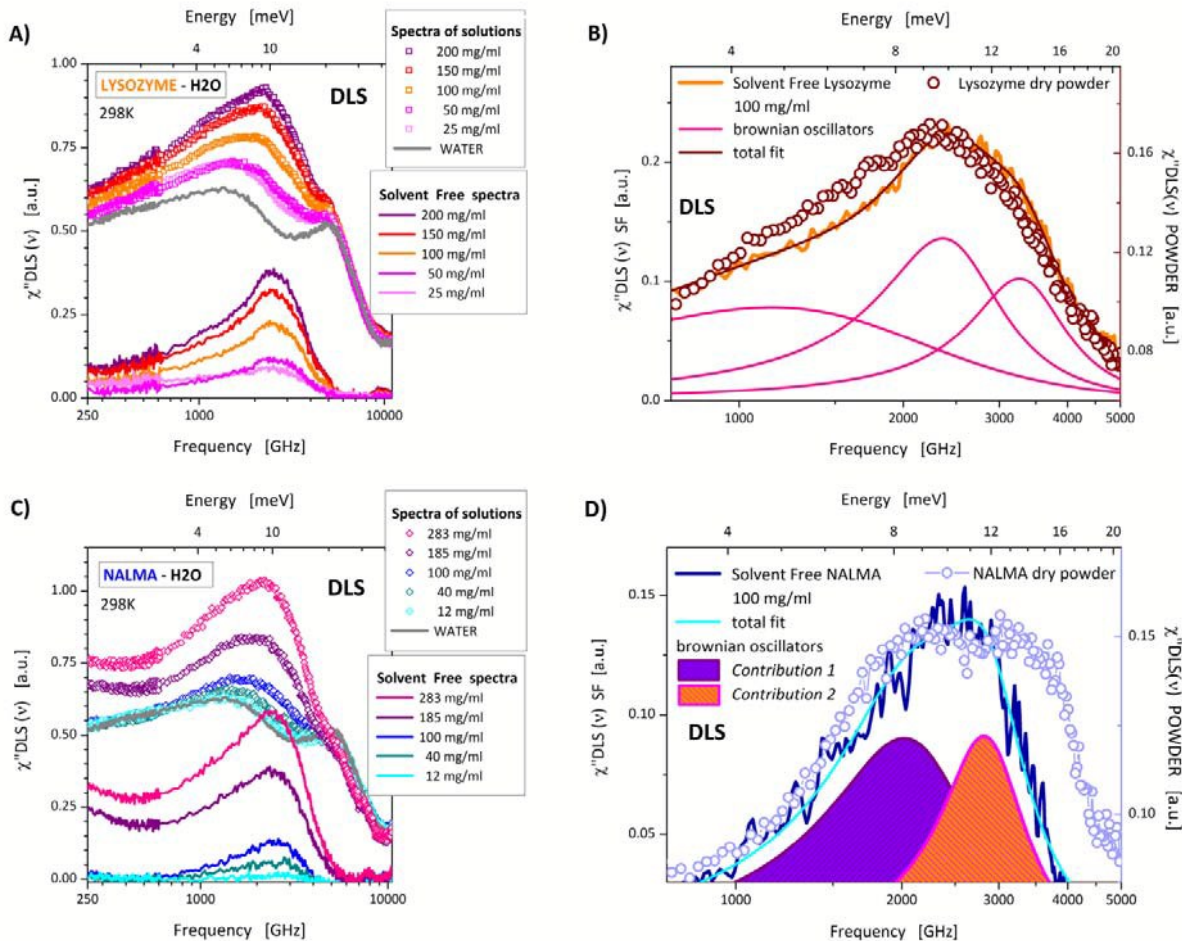


Figure 1 DLS low-frequency spectra of lysozyme (A-B) and NALMA (C-D) shown in logarithmic scale. A and C) Imaginary part of the DLS susceptibility of pure water (gray line) and biomolecule-water solutions (symbols) at different solute concentration ($T = 298\text{K}$). Spectra are rescaled to $\nu > 10^4$ GHz. SF_{DLS} obtained by subtracting the bulk solvent susceptibility (grey) from those of the solutions are displayed as continuous lines. B and D) SF_{DLS} distributions of 100 mg/ml lysozyme and NALMA solutions (continuous lines) are compared to the spectra of the corresponding dry powder (symbols) (298K). The spectra are normalized to the maximum height. The best fit and the Brownian oscillators curves obtained for the SF_{DLS} spectra^{8, 15} of lysozyme (three components) and NALMA (two components) are also shown.

Additional simulations of 50 ps (time step of 0.5 fs) at the same conditions have been performed to compute the VDOS. The program package nMOLDYN⁵³ (v.3.0.9) was used for the analysis of VDOS. Additional details can be found in the Electronic Supplementary Information.

Results and discussion

Complementary techniques are here employed to describe the low frequency vibrational properties of biomolecules. In particular we provide a set of comparisons to point out different aspects which are relevant for the vibrational dynamics of such systems. 1) We compare DLS spectra obtained for lysozyme and NALMA aqueous solutions to those of powders to highlight the influence of water on the low-frequency vibrations of the solute. 2) The molecular origin of the vibrational motions is investigated by comparison of DLS and NS spectra of lysozyme with those obtained for both dry powders and aqueous solutions of NALMA. 3) Finally, the internal

vibrational modes of NALMA and their contribution to the vibrational density of states are thoroughly determined using MD simulations.

Lysozyme and NALMA aqueous solutions and dry powders: DLS and NS data

DLS susceptibility spectra of lysozyme aqueous solutions collected at 298K are shown in Fig. 1A as a function of concentration. The data are rescaled to the librational band of water ($\nu > 10$ THz) as previously reported^{3, 8, 15}. Subtracting the spectrum of pure water from those of the protein solutions we obtain the solvent free, SF_{DLS} , profiles, highlighting the dynamics of the solute^{8, 15}. It has been shown that these SF distributions contain both solute contributions and solute-induced solvent changes below 300 GHz^{8, 15}.

The obtained SF_{DLS} profiles are consistent with the equivalent distributions obtained by OKE experiments^{3, 9}. We also compare the SF_{DLS} distribution of the 100 mg/ml lysozyme

solution with the spectrum observed for lysozyme dry powder at room temperature in Fig. 1B. Two points emerge from the SF_{DLS} spectra: (1) The integrated intensity of SF_{DLS} spectra between 600 and 5300 GHz linearly increases with solute concentration (Fig. S2 in Electronic Supplementary Information), whereas the shape of these profiles is essentially unaffected (Fig. 1A), and (2) the SF_{DLS} and hydrated powder data sets (Fig. 1B) show similar spectral features in this frequency range. On the basis of these observations, we can confidently assign the spectral contributions between ~300 and 5000 GHz to purely vibrational motions of the protein⁸. This vibrational contribution is indeed not sensitive to lysozyme aggregation effects⁵⁴.

A similar increase of the integrated area of the SF_{DLS} profiles is observed for the vibrational contribution of NALMA molecules in solution as a function of concentration (Fig. 1C). Comparison to NALMA in the powder state reveals that the vibrational distribution in solution is narrower than in powder state (Fig. 1D); moreover, it is also narrower than lysozyme. NALMA's SF_{DLS} feature can be well reproduced by two Brownian Oscillator (BO) functional forms¹⁵ peaked at 2050 (\pm 100) and 2820 (\pm 120) GHz (Fig. 1D), whereas lysozyme SF_{DLS} spectra require three BO curves to be used (Fig. 1B)^{8,9}. The component at lower frequencies in lysozyme spectrum accounts for the BP of the protein^{8,9}. The spectrum of NALMA dry powder shows two separated contributions of same intensity while, in solution these two features are less resolved. The lower frequency band of NALMA powder is located at a similar frequency (2120 \pm 110 GHz), but the second component is shifted to significantly higher energies in powder (3410 \pm 170 GHz) relative to the SF_{DLS} profile. The presence of a contribution of the peptide in this frequency range is consistent with a recent OKE experiment¹³. In that study, Mazur et al. observed the presence of a broad component located at ~2600 GHz in the frequency domain OKE spectra of a 0.5 M NALMA solution which they tentatively associated to vibrational motions in H-bonded solvated peptides solution¹³. NALMA in solution lacks the contribution around 1 THz, where the boson peak of lysozyme is observed.

This difference between the low frequency contributions of lysozyme and NALMA in solution is shown in more detail in Fig. 2. We now compare SF spectra of NALMA and lysozyme 100 mg/ml solutions at room temperature obtained with both DLS (Fig. 2A) and NS (Fig. 2B) techniques; spectra have been normalized to the maximum height. SF_{NS} profiles shown in Fig. 2B were obtained by taking the difference between the spectra of the solutions (hydrogenated lysozyme/D₂O and hydrogenated NALMA/D₂O) and the spectrum of pure D₂O, in an analogous treatment to DLS spectra. The effective volume occupied by the solutes in solution was considered during the subtraction as described in refs^{11,55}. Experimental limitations of DLS measurements on solid samples prevent the collection of spectra below 400 GHz; because of this, the BP of NALMA powder falls out of the experimental window for that technique, while it is observed in the high resolution NS spectra.

Low-frequency spectra of the protein and the peptide in powder state show the same contributions (Fig. 3). NALMA in a powder state does display a BP feature in the NS spectra, (Fig. 3), which appears at lower frequencies than the BP in lysozyme.

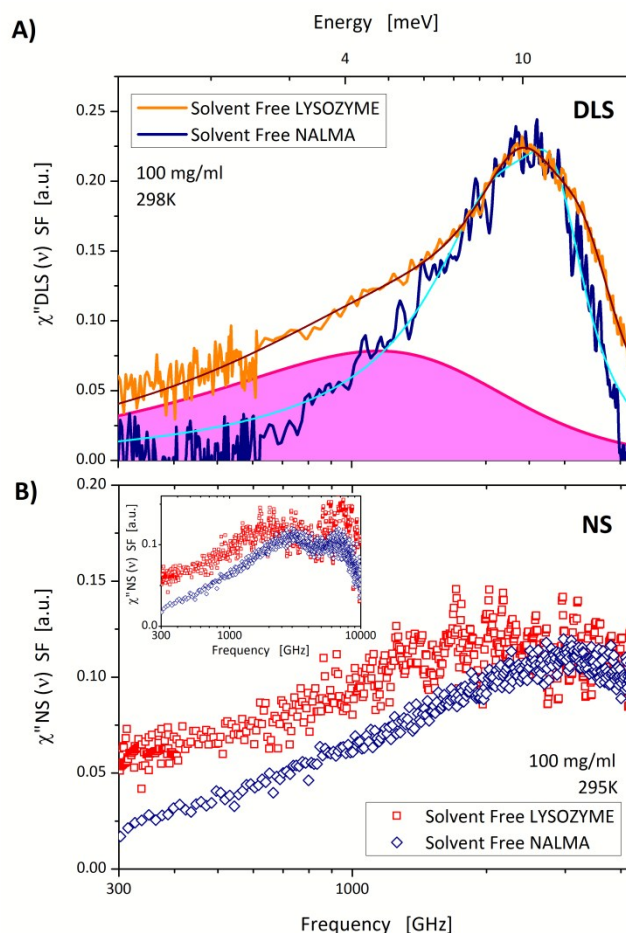


Figure 2 Solvent Free spectra in susceptibility formalism of NALMA (blue shades) and lysozyme (red shades) obtained at room temperature from DLS **A**) and NS **B**) data (100mg/ml solutions). Profiles were normalized to the intensities around the maximum at 2000-3000 GHz. Lysozyme boson peak obtained from the Multiple Brownian Oscillator curve fitting procedure⁸ is shown as pink colored area, together with the best fits (wine and cyan lines) obtained for the two systems^{8,15}. Panel **B** inset: SF_{NS} spectra are plotted in an extended frequency range up to 10 THz.

Fig. 3 shows the NS spectral densities $I_n(\nu)$ of dry NALMA and lysozyme powders together with the components of the fit, obtained using a Lorentzian functional form to reproduce the quasielastic scattering (QE) and a lognormal function for the boson peak (BP)^{36,37}. The BP position, ν_{BP} , obtained from the fit for NALMA and lysozyme dry powders at 295K is 169 (\pm 13) GHz and 518 (\pm 29) GHz respectively. We note that changing formalism from susceptibility (Figs. 1 and 2) to spectral density (Fig. 3), enhances the lower frequency side of the spectrum and shifts apparent spectral features, BP included, towards lower frequencies relative to the $\chi''(\nu)$ spectra⁵⁶. Why the BP is not present for NALMA in solution? The BP is observed in NS and DLS spectra of amino-acid mixtures powders^{21,37,38}, in glass forming systems⁴³⁻⁴⁵ and in proteins⁴⁰ at low and high temperature, in form of dry and hydrated powders as well as in solution. The answer lies in two points, (1) the size of NALMA molecule and (2) the nature of the BP motions themselves. The NALMA peptide has a molecular volume 179 \pm 12 Å³,^{15,57} and an approximate diameter ~7 Å.

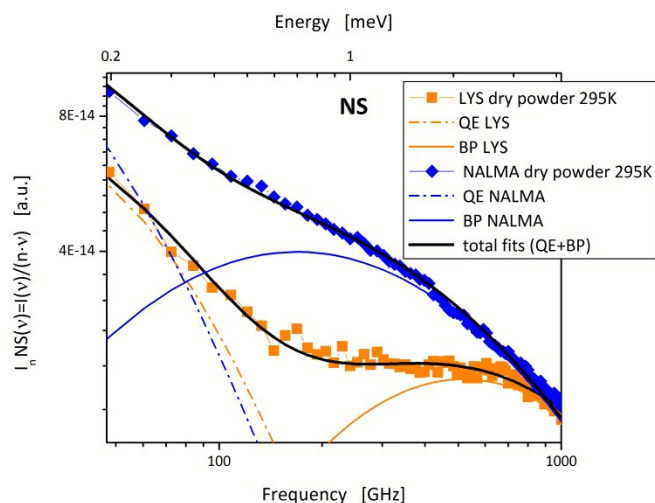


Figure 3 NS spectra of NALMA (diamonds) and lysozyme (squares) dry amorphous powders at 295K in the spectral density formalism. Components of the fit are also shown (lysozyme in orange and NALMA in blue): QE contributions are represented as dash-dot curves and BP contributions as continuous lines. Total fits are depicted in black.

This is important when we recall that the BP is connected to a characteristic length scale of heterogeneities in proteins ($\sim 1\text{--}2.5\text{ nm}$)³⁷ and glass forming networks. It follows that small molecules, such as NALMA, in solution are too small to exhibit BP collective vibrations because they are far below the size of the heterogeneities associated with these motions, and obviously too small to comprise networks of sufficient size to contain such heterogeneities. The BP reemerges in the powder sample of NALMA; where peptide molecules are capable of interacting with each other to form a disordered, glass-like network containing heterogeneities of the appropriate length scale, similar to amino-acid mixtures and small molecule glass formers.

The BP position can also be interpreted as a probe of rigidity of the system on the length scale of a few nanometers, with higher frequency correlating to a more rigid system³⁶. Our results from NALMA powders are therefore very interesting, as the BP position of NALMA at $169 (\pm 13)\text{ GHz}$ indicates the softest system yet observed within the context of proteins, amino acids, and protein analogues. The chemical nature of the NALMA peptide provides an explanation of this novel observation; consistent within the emerging picture from results on proteins and amino acid mixtures^{23, 36, 37}. NALMA is a relatively hydrophobic molecule, with methyl groups affecting the polar portion of the molecule and relatively few hydrogen bonding sites per molecule, when compared to most proteins and their constituent amino acid mixtures. This implies a lower number/strength of hydrogen bonds per volume when compared to these other systems. Amino acid mixtures corresponding to the sequence of a protein, on the other hand, are reported to have BPs at even higher frequencies than the folded protein ($\nu_{\text{BP}} = 785 \pm 24\text{ GHz}$ for the amino-acid mixture with composition of green fluorescent protein)^{37, 40}. Such mixtures of amino acids have a larger number and collective strength of H-bonds per residue from both amino and carboxyl groups being free to participate in the HB network. This observation on NALMA powder provides an additional

evidence in this emerging understanding of nanometer length scale rigidity; though we do not rule out the possibility of a contribution from damped vibrational modes at comparable frequencies.

A final point of interest emerges from the differences in spectral sensitivity between DLS and NS techniques in the frequency range of 5 to 10 THz for both protein and peptide samples. NS experiments show a clear vibrational component of the solutes above 5 THz (inset in Fig. 2B). The S_{DLS} spectra, on the other hand, have almost no solute contributions in the frequency range from 5 to 10 THz (Figs. 1A and 1C); with only residual intensity at high ($\sim 150\text{ mg/ml}$) solute concentration. Indeed the DLS spectra of protein and peptide solutions do not show any remarkable differences with the spectra of neat water in this frequency range. This piece of information helps to assign this specific feature to a physical motion which is active in one technique, but not in the other. We further support this with MD simulations, which provide a site-specific vibrational density of states (VDOS) as a function of hydration in order for NALMA. Together, this approach allows us to identify the motions corresponding to the peptide low frequency vibrations.

Dry and hydrated NALMA powders: MD simulations

VDOS of dry and hydrated NALMA ($h=0.68\text{ w/w}$) were computed from the stored trajectories (VDOS_{MD}). The total VDOS_{MD} calculated for dry NALMA closely resembles that extracted from NS experiments (VDOS_{NS}) (Fig. 4), showing two broad peaks below 10 THz. Fig. 4 also displays the decomposition of VDOS_{MD} based on the contributions of individual atoms, as obtained from the simulations. It appears that the vibrational features arise, almost entirely, from hydrogen atoms of methyl groups. Protons belonging to methyl groups of the polar backbone of the molecule (hydrogen atoms labelled HC2 and HC5) give coincident contributions to the VDOS_{MD} in this spectral region. Similarly, the components related to hydrogens (HC8 and HC9) of side-chain methyl groups located in the hydrophobic portion of the molecule are superimposed. However, due to their different positions within the NALMA molecule, these two pairs of methyl groups have distinct spectra with respect to each other as we observe in Fig. 4. This effect of microenvironment on methyl group dynamics is in agreement with previous findings on protein samples. Based on MD simulations on lysozyme samples, Lerbret et al. also report that the intensities around 7200–7800 GHz mainly arise from the protein methyl groups¹². In the case of myoglobin Krishnan et al. found a splitting and shift in peak position of the two bands of CH_3 vibrations that differs significantly among methyl groups, depending on the local environment²⁹. Our S_{NS} data show that NALMA is a remarkably faithful model to study protein methyl group vibrations, showing features comparable to those of lysozyme in the 5–10 THz range (Fig. 2B inset). We next assign these spectral features to particular vibrations involving the methyl groups of NALMA. A number of infrared and Raman studies on monosubstituted amides in both liquid and solid state suggested the presence of in-phase and out-of phase CCH_3 and NCH_3 methyl torsions in the 6900–9000 GHz frequency range^{58–61}.

Neutron scattering investigations on NMA have also shown a band at 4800 GHz that involves the motion of both methyl groups⁶². More recently, Smith and coworkers have analyzed

ARTICLE

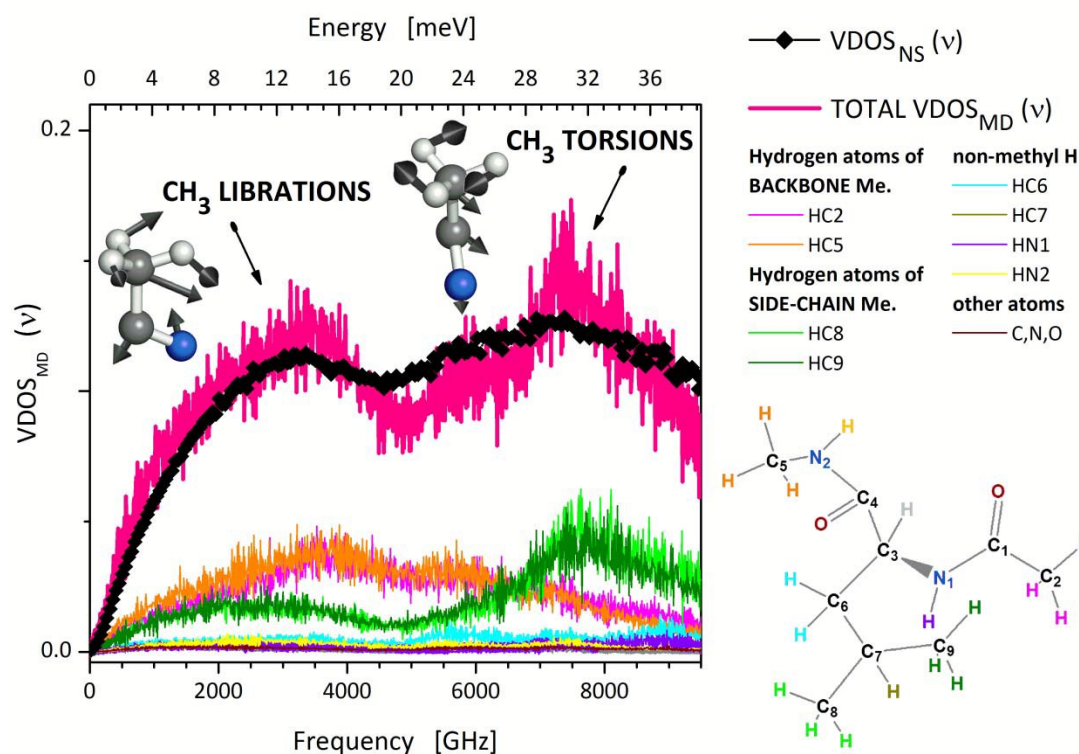


Figure 4 VDOS profiles at room temperature obtained from NS experiments (black diamonds) and MD simulations (pink line) on dry NALMA. These two VDOSs curves were normalized to the integral calculated over the frequency range up to 10 THz. Atomic contributions to VDOS_{MD} are shown in the same color adopted for the labeling of the peptide atoms (molecule scheme). Hydrogen atoms of backbone methyl groups are depicted in orange (HC5) and magenta (HC2); protons of side-chain methyl groups are shown in green (HC8) and olive (HC9) colors.

the VDOS of methyl groups from small molecules and proteins²⁹⁻³³, assigning the vibrational band observed between 1500–3750 GHz to a librational-type motion of the methyl hydrogens and the band around 6900–9300 GHz to hindered torsions of methyl groups²⁹. This suggests a preliminary assignment of NALMA vibrational modes in the 1–5 THz frequency range to methyl groups' librations; those between 5 and 10 THz to CH₃ hindered torsions. Our experimental and simulation results are consistent with the interpretation of two different classes of vibrations. This assignment of the high frequency component to CH₃ torsions explains the lack of intensity between 5 and 10 THz in all the DLS spectra of both NALMA and lysozyme. Hindered rotations do not modulate the polarizability of the molecule and therefore contribute weakly to the DLS spectrum, in contrast to NS (and MD) which are directly sensitive to the atomic motions of the hydrogen atoms, and therefore detect both methyl groups' types of vibrations. We remark that hindered torsions do not refer to the three-site jump rotations typically investigated by elastic neutron scattering and NMR experiments²⁵. Such relaxations occur at slower timescales (from tens to hundreds picoseconds in proteins^{14, 23}) than the hindered rotations of methyl groups discussed in this work. Site-specific results on three-site jumps methyl rotational relaxations of NALMA, which were extracted from our MD simulations, have been discussed in a previous publication⁶³. A schematic representation of the time scales corresponding to all relaxational and vibrational methyl groups'

dynamics of NALMA peptide, drawn on the basis of our experimental and simulated data, is reported in the Electronic Supplementary Information (Fig. S3).

An intriguing result concerning the methyl groups' torsions (Fig. 4) is the existence of two distinct dynamical populations in NALMA with spectral distributions of backbone (hydrophilic) and side-chain (hydrophobic) methyl groups peaked at ca. 5500 and 7500 GHz, respectively. Methyl groups located in the hydrophobic portion of the molecule show higher force constants and are more hindered than those in the more hydrophilic backbone.

Concerning the low frequency librational motions, MD simulations suggest that the main contribution around 3400 GHz is from hydrogen atoms of backbone methyl groups (Fig. 4). On the other hand, librations of both backbone and side chain CH₃ groups are responsible for the measured spectral density around 2000 GHz. These findings might be helpful also for the interpretation of DLS spectral features. Based on MD results, we can tentatively assign the high frequency component of DLS spectra of SF_{DLS} and dry powder (*Component 2*, Fig. 1D) mainly to librations of methyl groups directly bonded to the hydrophilic portion of the NALMA molecule, while the assignment of *Component 1* for the DLS spectra of NALMA (Fig. 1D and Fig. 4) in terms of dynamics of specific groups is less straightforward. Despite having a negligible contribution in VDOS_{NS/MD} (Fig. 4), the motions of other molecular groups might contribute significantly to the DLS spectrum of NALMA.

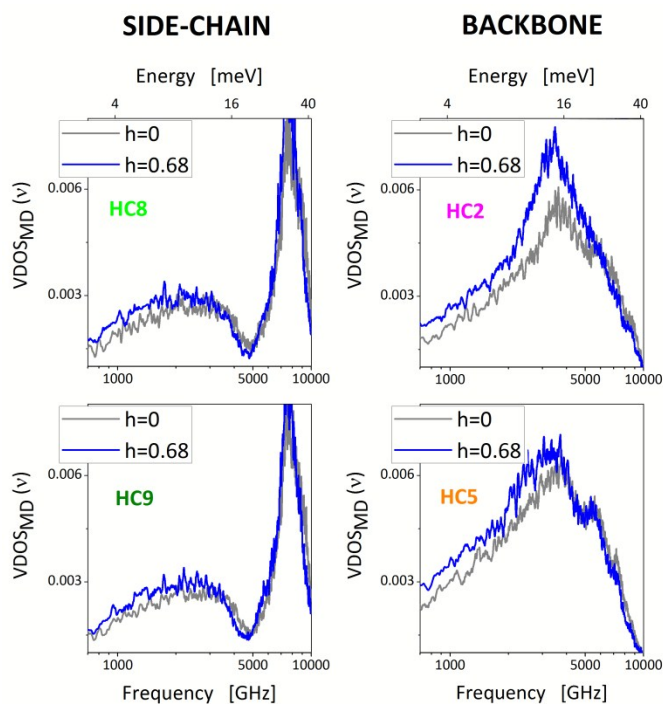


Figure 5 VDOS_{MD} of H atoms of side-chain (left) and backbone (right) methyl groups calculated for NALMA powders. In each plot the VDOS_{MD} of the same subset of methyl protons is shown for dry (gray) and h=0.68 hydrated (blue) NALMA at 298K.

below 5 THz, due to the delocalized character typically expected for low frequency vibrations.

To have a complete picture, the influence of the hydration was also investigated at room temperature. In Fig. 5 the contributions of backbone and side-chain methyl groups to VDOS_{MD} for the dry peptide are compared to those calculated for a powder hydrated at h=0.68. Methyl groups' librations show a strong influence from hydration. We observe a red shift of the VDOS distributions in the hydrated samples, with backbone methyl groups' librations showing lower force constants and less hindered motions relative to the dry powder state. The presence of water molecules has a plasticizing effect on the methyl groups of the hydrophilic backbone, creating a less hindered local environment and facilitating their librational motions. This trend is in agreement with DLS spectra depicted in Fig. 1D, where *Component 2* moves from 3410 GHz when dry, to lower frequencies (2820 GHz) in the solution state. Our results and interpretation might also explain previous OKE findings obtained for highly concentrated NALMA solutions that show a red shift of the peptide vibrational components from 2730 to 2600 GHz upon dilution (from 2M to 0.5 M)¹³.

On the other hand, methyl groups' torsions seem less affected by the presence of water. This is particularly evident for the methyl groups located in the hydrophobic portion of the molecule, which show a bigger separation between librational and torsional components.

Conclusions

Neutron and light scattering experiments have been used to examine the low frequency vibrations of a protein, lysozyme, and of a peptide, NALMA, in solution and in powder state. Our experimental results show that the low frequency vibrational spectrum of lysozyme, in solution and powder state reveals

similar distributions in the range of ~0.3–5 THz. This supports the validity of a large number of results within this frequency range, obtained using powder protein samples. In parallel, the experimental results on NALMA peptide depict a system which is simple enough to provide site sensitivity, while still exhibiting vibrational features resembling those observed in proteins. Our main finding concerns an intriguing difference between the spectra of NALMA in solution and in powder state. This difference can be ascribed to the boson peak which is present in NALMA powder and is not observed in NALMA solution. This result suggests that BP vibrations are related to a characteristic length scale of the heterogeneities present in the system. The size of NALMA molecules in solutions is smaller than the size of heterogeneities associated with boson peak collective vibrations. In powder state instead, NALMA molecules interact with each other and form a disordered network, which is comparable to those of amino-acid mixtures and small molecule glass formers, and contains heterogeneities of the appropriate length scale to manifest BP motions. This insight into the molecular origin of the BP in proteins might have significant implications for the biological activity of proteins.

In this context, MD simulations have represented a powerful complementary tool to identify the specific sites which are relevant for vibrational processes. In particular, our MD simulations reveal that the low frequency vibrations of NALMA between 1 and 10 THz can be ascribed exclusively to librations and hindered torsions of methyl groups. Methyl groups are thought to play an important role as intrinsic plasticizers favoring protein dynamics, flexibility and activity²⁸. Our data also show that such hindered torsions are not Raman active and that some of the low frequency vibrations of the peptide are more sensitive to the local environment relative to lysozyme. The spectra of NALMA in the powder state show a substantial blue shift of the librations of methyl groups located in the hydrophilic backbone of the molecule relative to NALMA in solution, along with the emergence of boson peak collective vibrations. These results further demonstrate the advantages to be gained from the use of simplified model systems. In this specific case, NALMA has proven to be an inspired choice, reproducing similar features to the low-frequency vibrational spectra of proteins.

Whether due to limitations of a technique or to the choice of a reductionist approach, biochemical and biophysical communities often study biomolecules in conditions far from the in vivo scenario. This work has also highlighted a number of shortcomings, and advantages, in the use of model conditions to study protein low-frequency vibrations; our analysis stands as an example of how a combination of experimental/simulation techniques is capable of placing results in a biologically relevant context.

Acknowledgements

S.P. acknowledges the Computing for Science (CS) group at Institut Laue-Langevin (Grenoble, France); M.P. acknowledges support from MIUR-PRIN 2010-2011. Research at the Spallation Neutron Source, Oak Ridge National Laboratory, was sponsored by the Scientific User Facilities Division, Office of Basic Energy Sciences, U. S. Department of Energy.

Notes and references

^a Joint Institute for Neutron Sciences, Oak Ridge National Laboratory, Oak Ridge, TN, 37831, USA. Email: spertica@utk.edu

- ^b Chemical and Materials Sciences Division, Oak Ridge National Laboratory, Oak Ridge, TN, 37831, USA.
- ^c Department of Chemistry, University of Tennessee, Knoxville, TN, 37996, USA.
- ^d CNR-IOM, Italy c/o Institut Laue Langevin, France. Email: russo@ill.fr
- ^e Institut Lumière Matière, Université de Lyon 1, France.
- ^f Dipartimento di Chimica, Biologia e Biotecnologia, Università di Perugia, Via Elce di Sotto 8, I-06123 Perugia, Italy.
- ^g Institut Laue Langevin, 6 rue J. Horowitz BP156, F-38042 Grenoble, France.
- ^h Quantum Condensed Matter Division, Oak Ridge National Laboratory, PO Box 2008, Oak Ridge, TN, 37831, USA.
- ⁱ IOM-CNR c/o Dipartimento di Fisica e Geologia, Università di Perugia, Via Pascoli, I-06123 Perugia, Italy.
- ^j Dipartimento di Fisica e Geologia, Università di Perugia, Via Pascoli, I-06123 Perugia, Italy.
- ^k Centro di Eccellenza sui Materiali Innovativi Nanostrutturati (CEMIN), Università di Perugia, Via Elce di Sotto 8, I-06123 Perugia, Italy.
- † Electronic Supplementary Information (ESI) available: Additional details on MD simulations; integrated intensity of SF_{DLS} spectra of lysozyme; graphical summary of methyl groups' dynamics of hydrated NALMA powders from MD simulations. See DOI: 10.1039/b000000x/
- H. Frauenfelder, S. G. Sligar and P. G. Wolynes, *Science*, 1991, **254**, 1598.
 - E. Balog, T. Becker, M. Oettl, R. Lechner, R. Daniel, J. Finney and J. C. Smith, *Physical review letters*, 2004, **93**, 028103.
 - D. A. Turton, H. M. Senn, T. Harwood, A. J. Laphorn, E. M. Ellis and K. Wynne, *Nature Communications*, 2014, **5**, 3999.
 - S. D. Schwartz and V. L. Schramm, *Nature chemical biology*, 2009, **5**, 551.
 - O. Marques and Y. H. Sanejouand, *Proteins: Structure, Function, and Bioinformatics*, 1995, **23**, 557.
 - S. Hammes-Schiffer, *Biochemistry*, 2002, **41**, 13335.
 - M. Gruebele and D. Thirumalai, *The Journal of Chemical Physics*, 2013, **139**, 121701.
 - S. Perticaroli, L. Comez, M. Paolantoni, P. Sassi, L. Lupi, D. Fioretto, A. Paciaroni and A. Morresi, *The Journal of Physical Chemistry B*, 2010, **114**, 8262.
 - G. Giraud, J. Karolin and K. Wynne, *Biophysical journal*, 2003, **85**, 1903.
 - P. Sassi, S. Perticaroli, L. Comez, A. Giugliarelli, M. Paolantoni, D. Fioretto and A. Morresi, *The Journal of Chemical Physics*, 2013, **139**, 225101.
 - M. Marconi, E. Cornicchi, G. Onori and A. Paciaroni, *Chemical Physics*, 2008, **345**, 224.
 - A. Lerbret, F. Affouard, P. Bordat, A. Hedoux, Y. Guinet and M. Descamps, *The Journal of Chemical Physics*, 2009, **131**, 245103.
 - K. Mazur, I. A. Heisler and S. R. Meech, *The Journal of Physical Chemistry B*, 2010, **114**, 10684.
 - L. Hong, D. C. Glass, J. D. Nickels, S. Perticaroli, Z. Yi, M. Tyagi, H. O'Neill, Q. Zhang, A. P. Sokolov and J. C. Smith, *Physical review letters*, 2013, **110**, 028104.
 - S. Perticaroli, L. Comez, M. Paolantoni, P. Sassi, A. Morresi and D. Fioretto, *Journal of the American Chemical Society*, 2011, **133**, 12063.
 - C. Andreani, A. Deriu, A. Filabozzi and D. Russo, *Physica B: Condensed Matter*, 1997, **234**, 223.
 - D. Russo, J. Pérez, M. Desmadril, P. Calmettes and D. Durand, *Physica B: Condensed Matter*, 2000, **276**, 499.
 - M. G. Ortore, F. Spinozzi, P. Mariani, A. Paciaroni, L. R. Barbosa, H. Amenitsch, M. Steinhart, J. Ollivier and D. Russo, *Journal of The Royal Society Interface*, 2009, rsif20090163.
 - A. Filabozzi, A. Deriu, M. Di Bari, D. Russo, S. Croci and A. Di Venere, *Biochimica et Biophysica Acta (BBA)-Proteins and Proteomics*, 2010, **1804**, 63.
 - D. Russo, J. Teixeira and J. Ollivier, *The Journal of Chemical Physics*, 2009, **130**, 235101.
 - M. Diehl, W. Doster, W. Petry and H. Schober, *Biophysical journal*, 1997, **73**, 2726.
 - D. Russo, E. Pellegrini, M. A. Gonzalez, S. Perticaroli and J. Teixeira, *Chemical Physics Letters*, 2011, **517**, 80.
 - S. Perticaroli, J. D. Nickels, G. Ehlers, E. Mamontov and A. P. Sokolov, *The journal of physical chemistry. B*, 2014, **118**, 7317–7326.
 - J. E. Curtis, M. Tarek and D. J. Tobias, *Journal of the American Chemical Society*, 2004, **126**, 15928.
 - T. I. Igumenova, K. K. Frederick and A. J. Wand, *Chemical Reviews*, 2006, **106**, 1672.
 - R. B. Best, T. J. Rutherford, S. M. V. Freund and J. Clarke, *Biochemistry*, 2004, **43**, 1145.
 - O. Millet, A. Mittermaier, D. Baker and L. E. Kay, *Journal of molecular biology*, 2003, **329**, 551.
 - J. D. Nickels, J. E. Curtis, H. O'Neill and A. P. Sokolov, *Journal of biological physics*, 2012, **38**, 497.
 - M. Krishnan, V. Kurkal-Siebert and J. C. Smith, *The Journal of Physical Chemistry B*, 2008, **112**, 5522.
 - A. V. Goupil-Lamy, J. C. Smith, J. Yunoki, S. F. Parker and M. Kataoka, *Journal of the American Chemical Society*, 1997, **119**, 9268.
 - N.-D. Morelon, G. R. Kneller, M. Ferrand, A. Grand, J. C. Smith and M. Bée, *The Journal of Chemical Physics*, 1998, **109**, 2883.
 - C. Hartmann, M. Joyeux, H. P. Trommsdorff, J. C. Vial and C. von Borczyskowski, *The Journal of Chemical Physics*, 1992, **96**, 6335.
 - R. Hayward, H. Middendorf, U. Wanderlingh and J. Smith, *The Journal of Chemical Physics*, 1995, **102**, 5525.
 - V. Kurkal-Siebert and J. C. Smith, *Journal of the American Chemical Society*, 2006, **128**, 2356.
 - J. D. Nickels, S. Perticaroli, H. O'Neill, Q. Zhang, G. Ehlers and A. P. Sokolov, *Biophysical journal*, 2013, **105**, 2182.
 - S. Perticaroli, J. D. Nickels, G. Ehlers, H. O'Neill, Q. Zhang and A. P. Sokolov, *Soft Matter*, 2013, **9**, 9548.
 - S. Perticaroli, J. D. Nickels, G. Ehlers and A. P. Sokolov, *Biophysical journal*, 2014, **106**, 2667.
 - G. Schiro, C. Caronna, F. Natali, M. M. Koza and A. Cupane, *The Journal of Physical Chemistry Letters*, 2011, **2**, 2275.
 - M. Tarek and D. J. Tobias, *The Journal of Chemical Physics*, 2001, **115**, 1607.
 - J. D. Nickels, H. O'Neill, L. Hong, M. Tyagi, G. Ehlers, K. L. Weiss, Q. Zhang, Z. Yi, E. Mamontov and J. C. Smith, *Biophysical journal*, 2012, **103**, 1566.

- 41 J. D. Nickels, V. García Sakai and A. P. Sokolov, *The Journal of Physical Chemistry B*, 2013, **117**, 11548.
- 42 J. Roh, J. Curtis, S. Azzam, V. Novikov, I. Peral, Z. Chowdhuri, R. Gregory and A. Sokolov, *Biophysical journal*, 2006, **91**, 2573.
- 43 V. Malinovsky, V. Novikov, P. Parshin, A. Sokolov and M. Zemlyanov, *EPL (Europhysics Letters)*, 1990, **11**, 43.
- 44 A. Sokolov, R. Calemczuk, B. Salce, A. Kisliuk, D. Quitmann and E. Duval, *Physical review letters*, 1997, **78**, 2405.
- 45 U. Buchenau, A. Wischnewski, D. Richter and B. Frick, *Physical review letters*, 1996, **77**, 4035.
- 46 D. Russo, J. Teixeira, L. Kneller, J. R. Copley, J. Ollivier, S. Perticaroli, E. Pellegrini and M. A. Gonzalez, *Journal of the American Chemical Society*, 2011, **133**, 4882.
- 47 D. Russo, J. Ollivier and J. Teixeira, *Physical Chemistry Chemical Physics*, 2008, **10**, 4968.
- 48 G. Ehlers, A. A. Podlesnyak, J. L. Niedziela, E. B. Iverson and P. E. Sokol, *Review of Scientific Instruments*, 2011, **82**, 085108.
- 49 R. T. Azuah, L. R. Kneller, Y. Qiu, P. L. Tregenna-Piggott, C. M. Brown, J. R. Copley and R. M. Dimeo, *Journal of Research of the National Institute of Standards and Technology*, 2009, **114**, 341.
- 50 A. Sokolov, U. Buchenau, W. Steffen, B. Frick and A. Wischnewski, *Physical Review B*, 1995, **52**, R9815.
- 51 M. Bée and M. Bee, *Quasielastic neutron scattering: principles and applications in solid state chemistry, biology and materials science*, Adam Hilger Bristol, 1988.
- 52 v. Materials Studio Modelling Environment, Accelrys Inc., , San Diego (2009).
- 53 T. Róg, K. Murzyn, K. Hinsén and G. R. Kneller, *Journal of computational chemistry*, 2003, **24**, 657.
- 54 S. Perticaroli, L. Comez, P. Sassi, M. Paolantoni, S. Corezzi, S. Caponi, A. Morresi and D. Fioretto, *Journal of Non-Crystalline Solids*, 2014, doi:10.1016/j.jnoncrysol.2014.07.017.
- 55 J. Pérez, J.-M. Zanotti and D. Durand, *Biophysical journal*, 1999, **77**, 454.
- 56 V. Novikov, A. Sokolov, B. Strube, N. Surovtsev, E. Duval and A. Mermet, *The Journal of Chemical Physics*, 1997, **107**, 1057.
- 57 L. Comez, S. Perticaroli, M. Paolantoni, P. Sassi, S. Corezzi, A. Morresi and D. Fioretto, *Physical Chemistry Chemical Physics*, 2014, **16**, 12433.
- 58 F. Fillaux, M. Baron, C. De Loze and G. Sagon, *Journal of Raman Spectroscopy*, 1978, **7**, 244.
- 59 G. Kearley, M. Johnson, M. Plazanet and E. Suard, *The Journal of Chemical Physics*, 2001, **115**, 2614.
- 60 J. Durig, S. Craven and J. Bragin, *The Journal of Chemical Physics*, 1970, **52**, 2046.
- 61 J. Durig, S. Craven, J. Mulligan, C. Hawley and J. Bragin, *The Journal of Chemical Physics*, 1973, **58**, 1281.
- 62 F. Fillaux and J. Tomkinson, *Chemical Physics*, 1977, **26**, 295.
- 63 D. Russo, M. A. Gonzalez, E. Pellegrini, J. Combet, J. Ollivier and J. Teixeira, *The Journal of Physical Chemistry B*, 2013, **117**, 2829.